# Predictive Models of Gas Sorption in a Metal–Organic Framework with Open-Metal Sites and Small Pore Sizes

Tony Pham,[†,§] Katherine A. Forrest,[†,§] Douglas M. Franz,[†] Zhiyong Guo,[‡] Banglin Chen,[⊥] and Brian Space*[,†]
[†]*Department of Chemistry, University of South Florida,*
*4202 East Fowler Avenue, CHE205, Tampa, Florida 33620-5250, United States*
[‡]*College of Material Science and Engineering, Fuzhou University,*
*Fuzhou, Fujian 350108, China*
[⊥]*Department of Chemistry, University of Texas at San Antonio,*
*One UTSA Circle, San Antonio, Texas 78249-0698, United States*
[§]Authors contributed equally
*brian.b.space@gmail.com

## Partial Charges

Inspection of the crystal structure for UTSA-20 revealed 14 atoms in chemically distinguishable environments (Figure S1). The partial charges for the various chemically distinct atoms in UTSA-20 were determined through electronic structure calculations on different representational fragments that were taken from the crystal structure of the MOF. Three fragments were considered for the calculations in this work and they are shown in Figure S2.

The NWChem *ab initio* simulation software[1] was used to calculate the electrostatic potential surface (ESP) of the each fragment. For these calculations, all C, H, and O atoms were treated with the 6-31G* basis set to produce overpolarized charges that are appropriate for condensed phase simulation,[2] while the LANL2DZ ECP basis set[3–5] was assigned to the $Cu^{2+}$ ions for proper treatment of the core electrons of this species. The CHELPG method[6] was used to fit the charges onto the atomic centers of each fragment to reproduce the respective ESPs. The calculated average partial charges for each chemically distinct atom within the fragments are provided in Table S1. We note that atoms that are located on the edges of the fragment were not included in the averaging.

The partial charges for all chemically distinct atoms were averaged between the fragments. It can be observed that excellent agreement was obtained for the partial charges for the unique atoms between the fragments, with standard deviations of no greater than 0.02 (see Table 1). When considering the average partial charges for the chemically distinct atoms between the fragments and the number of each type of atom within the unit cell, the calculated total charge of the system was not neutral. Since the magnitude of the total positive charge outweights the magnitude of the total negative charge in this case, all unique atoms with negative charges were multiplied by a factor (a ratio between the total positive and negative charges) to bring the magnitude of the total negative charge to be equivalent with that for the total negative charge. The resulting partial charges for each chemically distinct atom in UTSA-20 after the adjustment can be found in Table S2. These partial charges were used for the simulations in this work to calculate stationary electrostatic interactions.

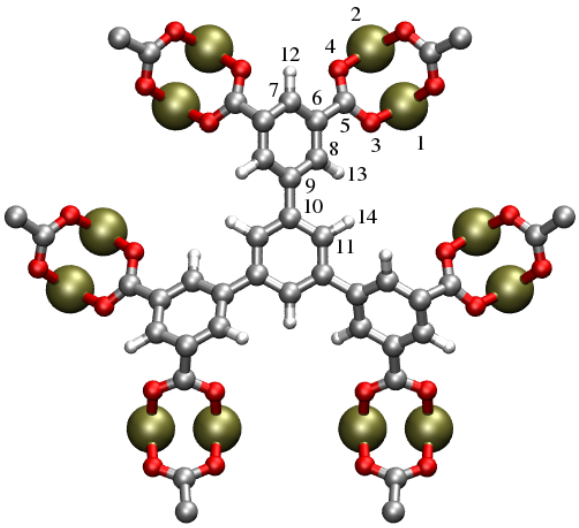


**Figure S1.** The numbering of the chemically distinct atoms in UTSA-20 as referred to in Tables S1 and S2. Atom colors: C = gray, H = white, O = red, Cu = tan.

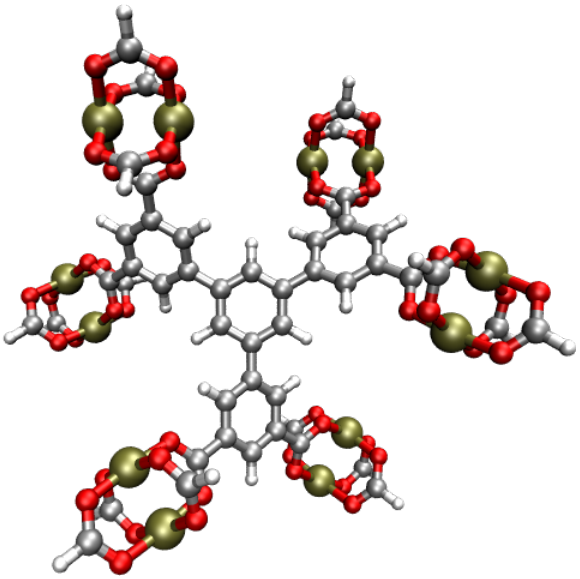

(a) Fragment 1

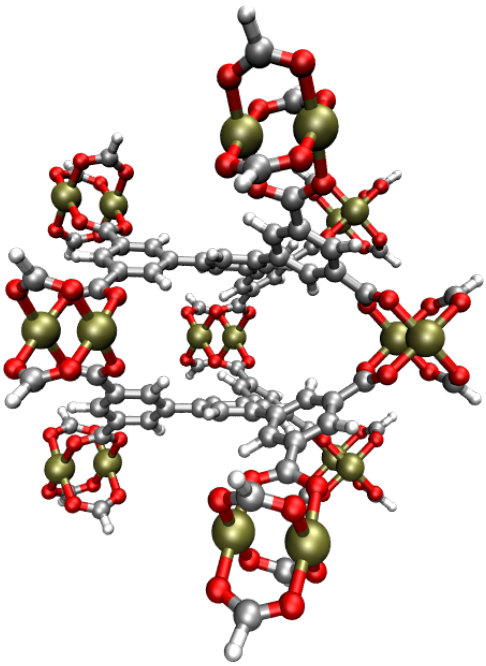

(b) Fragment 2

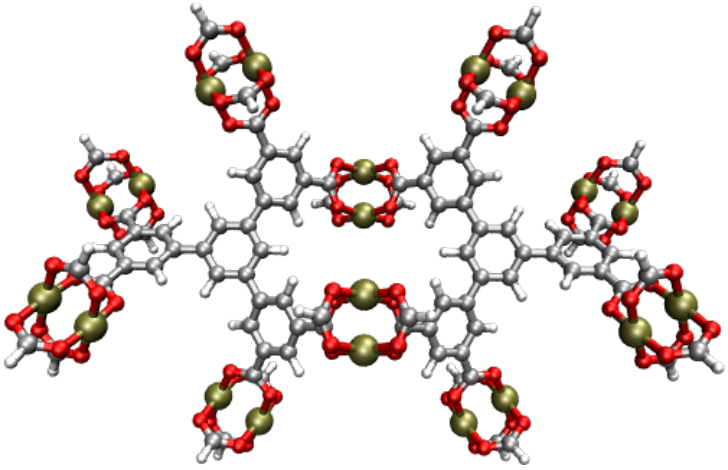

(c) Fragment 3

**Figure S2.** Fragments of UTSA-20 that were selected for gas phase charge fitting calculations. Atom colors: C = gray, H = white, O = red, Cu = tan.

**Table S1.** Calculated average partial charges ($e^-$) for the various chemically distinct atoms for the fragments that were selected for UTSA-20. The average and standard deviation (STD) between the fragments are also included. Labeling of atoms and fragments correspond to Figures S1 and S2, respectively.

| Atom | Label | Fragment 1 | Fragment 2 | Fragment 3 | Average | STD |
|---|---|---|---|---|---|---|
| Cu | 1 | 1.3405 | 1.3021 | 1.3186 | 1.3204 | 0.0193 |
| Cu | 2 | 0.8877 | 0.8971 | 0.8927 | 0.8925 | 0.0047 |
| O | 3 | -0.6839 | -0.6732 | -0.6807 | -0.6793 | 0.0055 |
| O | 4 | -0.7333 | -0.7402 | -0.7297 | -0.7344 | 0.0053 |
| C | 5 | 0.8879 | 0.8931 | 0.8776 | 0.8862 | 0.0079 |
| C | 6 | -0.0877 | -0.0905 | -0.0761 | -0.0847 | 0.0076 |
| C | 7 | -0.1255 | -0.1289 | -0.1341 | -0.1295 | 0.0043 |
| C | 8 | -0.1273 | -0.1235 | -0.1324 | -0.1277 | 0.0045 |
| C | 9 | 0.0421 | 0.0251 | 0.0445 | 0.0373 | 0.0106 |
| C | 10 | 0.1150 | 0.1247 | 0.1170 | 0.1189 | 0.0051 |
| C | 11 | -0.2703 | -0.2783 | -0.2731 | -0.2739 | 0.0041 |
| H | 12 | 0.2134 | 0.2186 | 0.2160 | 0.2160 | 0.0026 |
| H | 13 | 0.1438 | 0.1423 | 0.1473 | 0.1445 | 0.0026 |
| H | 14 | 0.1747 | 0.1780 | 0.1744 | 0.1757 | 0.0020 |

**Table S2.** The partial charges ($e^-$) for the chemically distinct atoms in UTSA-20 that were used for the simulations in this work. These were obtained by adjusting the average partial charges for the unique atoms between the fragments as shown in Table S1 to achieve system neutrality. The number of each type of atom within a unit cell of the MOF is also included. Label of atoms correspond to Figure S1.

| Atom | Label | # in Unit Cell | $q$ ($e^-$) |
|---|---|---|---|
| Cu | 1 | 6 | 1.3205 |
| Cu | 2 | 6 | 0.8925 |
| O | 3 | 24 | -0.6905 |
| O | 4 | 24 | -0.7465 |
| C | 5 | 24 | 0.8862 |
| C | 6 | 24 | -0.0861 |
| C | 7 | 12 | -0.1316 |
| C | 8 | 24 | -0.1298 |
| C | 9 | 12 | 0.0373 |
| C | 10 | 12 | 0.1189 |
| C | 11 | 12 | -0.2784 |
| H | 12 | 12 | 0.2160 |
| H | 13 | 24 | 0.1445 |
| H | 14 | 12 | 0.1757 |

## Experimental Isosteric Heat of Adsorption

### A. Virial Method

The experimental $CO_2$ and $H_2$ $Q_{st}$ values for UTSA-20 were determined for a range of loadings by applying the virial method[7,8] to the experimental sorption isotherms at different tmperatures (270 and 300 K for $CO_2$; 77, 87, 100 and 125 K for $H_2$). The isotherm data were simultaneously fitted to the following equation for the respective sorbates:

$$\ln P = \ln N + \left(\frac{1}{T}\right)\sum_{i=0}^{m} a_i N^i + \sum_{j=0}^{n} b_j N^j \tag{1}$$

where $P$ is the pressure (in atm), $N$ is the amount sorbed (in mmol $g^{-1}$), $T$ is the temperature (in K), $a_i$ and $b_i$ are the temperature-independent virial coefficients, and $m$ and $n$ represent the number of coefficients required to fit the isotherm data. The equation was fit using the $R$ statistical software package.[9] The values of the virial coefficients $a_0$ through $a_m$ were then used to calculate the $Q_{st}$ using the following equation:

$$Q_{st} = -R\sum_{i=0}^{m} a_i N^i \tag{2}$$

where $R$ is the ideal gas constant. The parameters that were obtained through virial fitting of the experimental isotherms for $CO_2$ and $H_2$ in UTSA-20 are provided in Table S3.

**Table S3.** Parameters that were obtained through virial fitting of the experimental $CO_2$ and $H_2$ sorption isotherms for UTSA-20.

| Parameter | $CO_2$ | $H_2$ |
|---|---|---|
| $a_0$ | -1888.26676127194 | -849.629877095545 |
| $a_1$ | 87.6487960589942 | 4.59981303275264 |
| $a_2$ | -8.18781257911261 | 4.29276575796839 |
| $a_3$ | -2.35142360743137 | -0.74436348539854 |
| $a_4$ | 0.17750969426114 | 0.0446638055582379 |
| $a_5$ | -0.00414556424663228 | -0.000862998910795889 |
| $b_0$ | 4.17052943361509 | 5.80696533539639 |
| $b_1$ | -0.299814617814247 | -0.0303864575455901 |
| $b_2$ | 0.0724185117483609 | 0.00717110861062452 |

### B. Dual-Site Langmuir–Freundlich Method

The experimental $CO_2$ $Q_{st}$ for UTSA-20 were also determined through the dual-site Langmuir–Freundlich (DSLF) method.[10] Here, the experimental excess $CO_2$ sorption isotherms at 270 and 300 K were simultaneously fitted to the DSLF equation:[11]

$$n = \frac{n_{m1} b_1 P^{\left(\frac{1}{t_1}\right)}}{1 + b_1 P^{\left(\frac{1}{t_1}\right)}} + \frac{n_{m2} b_2 P^{\left(\frac{1}{t_2}\right)}}{1 + b_2 P^{\left(\frac{1}{t_2}\right)}} \tag{3}$$

where $n$ is the gas uptake (in mmol g$^{-1}$), $P$ is the pressure of the bulk gas at equilibrium with the sorbed phase (in kPa), $n_{m1}$, $b_1$, and $t_1$ are the saturation uptake (in mmol g$^{-1}$), the affinity coefficient (in kPa$^{-1}$), and the deviation from the ideal homogeneous surface (unitless) for site 1, respectively, and $n_{m2}$, $b_2$, and $t_2$ are analogous parameters for site 2. Furthermore, $b_1$ and $b_2$ are expressed as a function of temperature *via* the following:

$$b_1 = b_{01} e^{\left(\frac{E_1}{RT}\right)} \tag{4}$$

$$b_2 = b_{02} e^{\left(\frac{E_2}{RT}\right)} \tag{5}$$

where $R$ is the ideal gas constant, $b_{01}$ and $E_1$ are the pre-exponential factor (in kPa$^{-1}$) and the activation energy (in kJ mol$^{-1}$) for site 1, and $b_{02}$ and $E_2$ are analogous parameters for site 2. The parameters obtained for the simultaneous fitting of the experimental $CO_2$ sorption isotherms at 270 and 300 K in UTSA-20 are provided in Table S4. These parameters were used to calculate the $Q_{st}$ values for a range of uptakes using the Clausius–Clapeyron equation:[12]

$$Q_{st} = \frac{R T_1 T_2}{T_2 - T_1} \ln\left(\frac{P_1}{P_2}\right) \tag{6}$$

where $T_1$ and $T_2$ are the two different temperatures (in K), and $P_1$ and $P_2$ are the corresponding pressures (in kPa) that were calculated for a range of uptakes using the temperature-dependent DSLF equation through the Newton–Raphson method.[13]

**Table S4.** Parameters for the temperature-dependent dual-site Langmuir-Freundlich (DSLF) equation for simultaneously fitting the experimental excess $CO_2$ sorption isotherms at 270 K and 300 K in UTSA-20. The $R^2$ value is also provided.

| Parameter | Value |
|---|---|
| $n_{m1}$ (mmol g$^{-1}$) | 11.1168558766339 |
| $b_{01}$ (kPa$^{-1}$) | 6.1585520487259E-07 |
| $t_1$ | 0.78270414219155 |
| $E_1$ (kJ mol$^{-1}$) | 19.5202763243779 |
| $n_{m2}$ (mmol g$^{-1}$) | 20.2600671402611 |
| $b_{02}$ (kPa$^{-1}$) | 5.91624923360022E-07 |
| $t_2$ | 2.42532343496328 |
| $E_2$ (kJ mol$^{-1}$) | 23.6110728846 |
| $R^2$ | 0.995893619276439 |

**Simulated $CO_2$ Sorption Results**

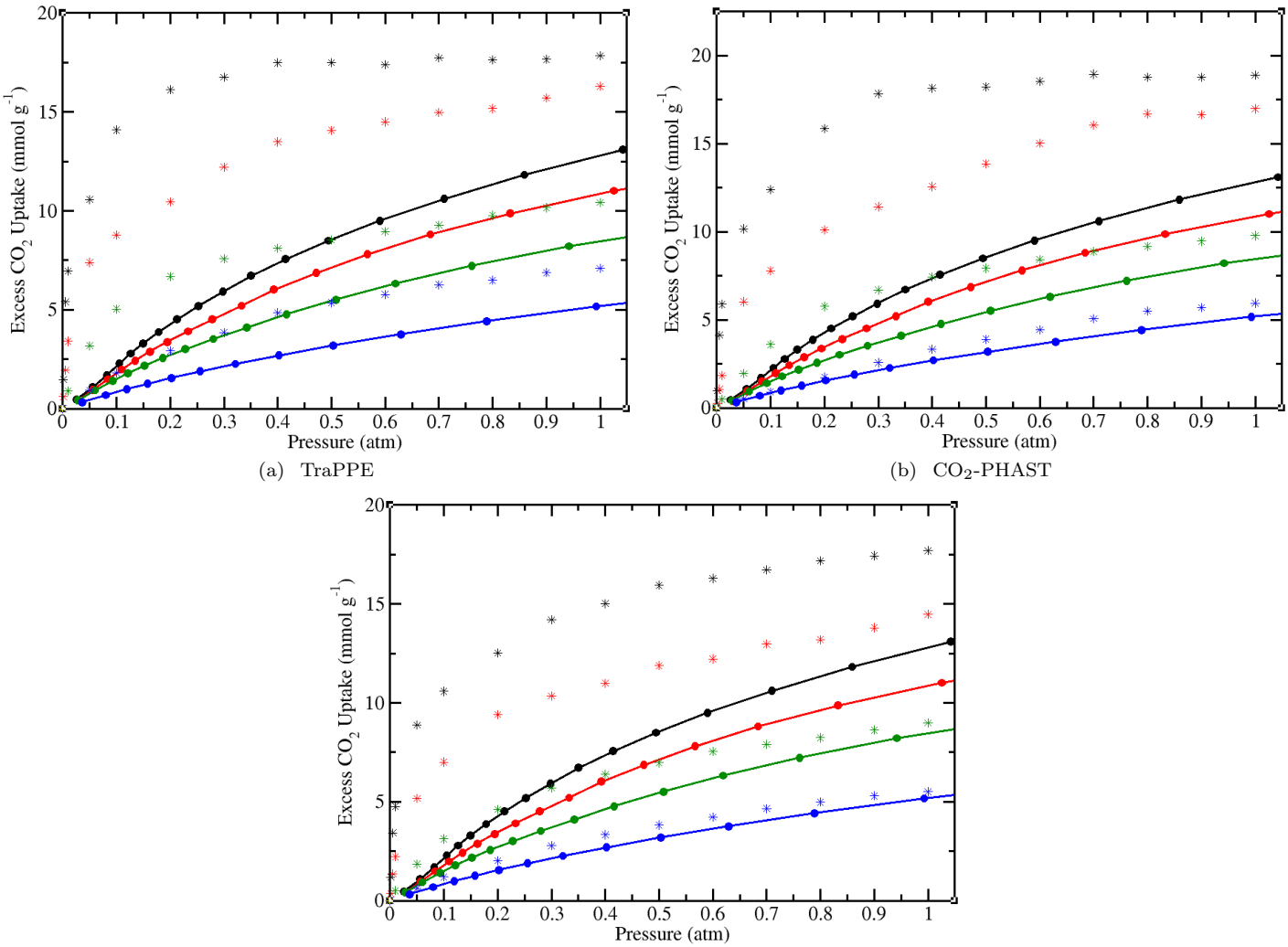


(a) TraPPE

(b) $CO_2$-PHAST

(c) $CO_2$-PHAST*

**Figure S3.** Low pressure (up to 1 atm) excess $CO_2$ sorption isotherms in UTSA-20 for experiment (circles with lines) and simulation (star) at 220 K (black), 240 K (red), 270 K (green), and 300 K (blue). The simulated results are shown for the **(a)** TraPPE, **(b)** $CO_2$-PHAST, and **(c)** $CO_2$-PHAST* models. The experimental data were taken from reference 14.

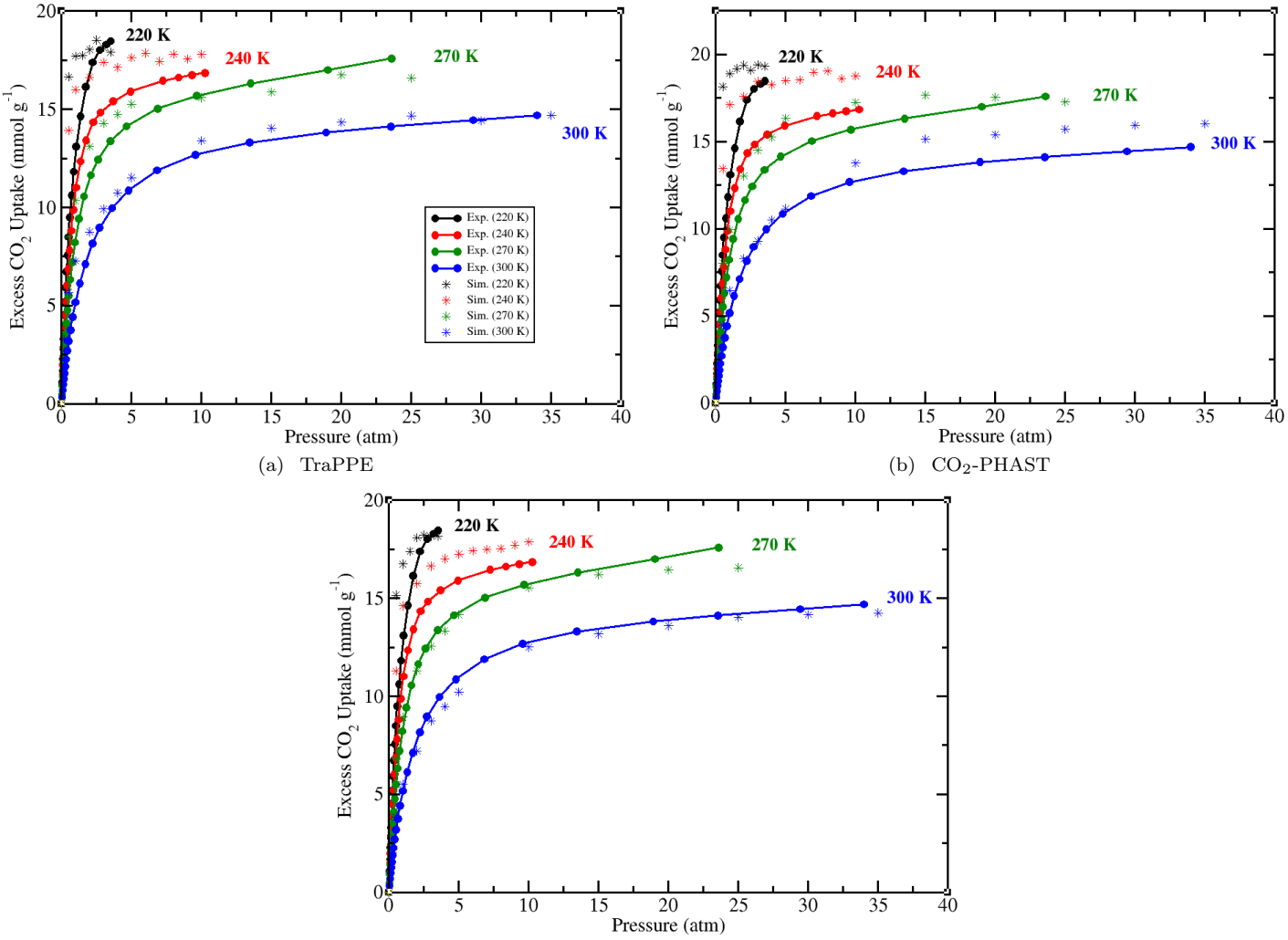


(a) TraPPE

(b) $CO_2$-PHAST

(c) $CO_2$-PHAST*

**Figure S4.** High pressure excess $CO_2$ sorption isotherms in UTSA-20 for experiment (circles with lines) and simulation (star) at 220 K (black), 240 K (red), 270 K (green), and 300 K (blue). The simulated results are shown for the **(a)** TraPPE, **(b)** $CO_2$-PHAST, and **(c)** $CO_2$-PHAST* models. The experimental data were taken from reference 14.

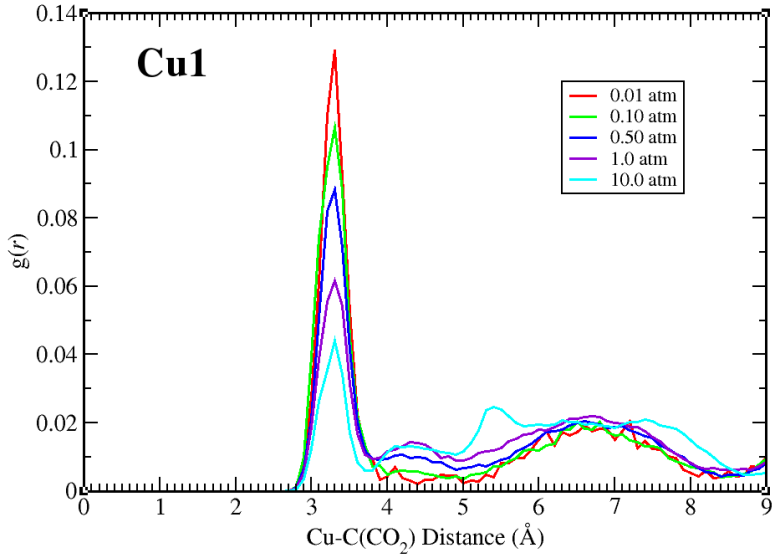


(a)

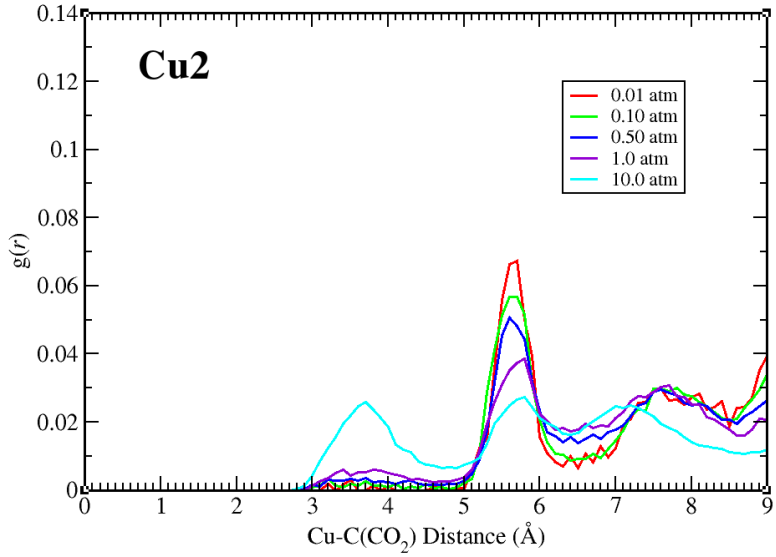


(b)

**Figure S5.** Radial distribution function (g($r$)) of $CO_2$ carbon atoms about **(a)** the Cu1 ions (atom label 1 in Figure S1) and **(b)** the Cu2 ions (atom label 2 in Figure S1) in UTSA-20 for simulations using the $CO_2$-PHAST* model at 300 K and 0.01 (red), 0.10 (green), 0.50 (blue), 1.0 (violet), and 10.0 atm (cyan).

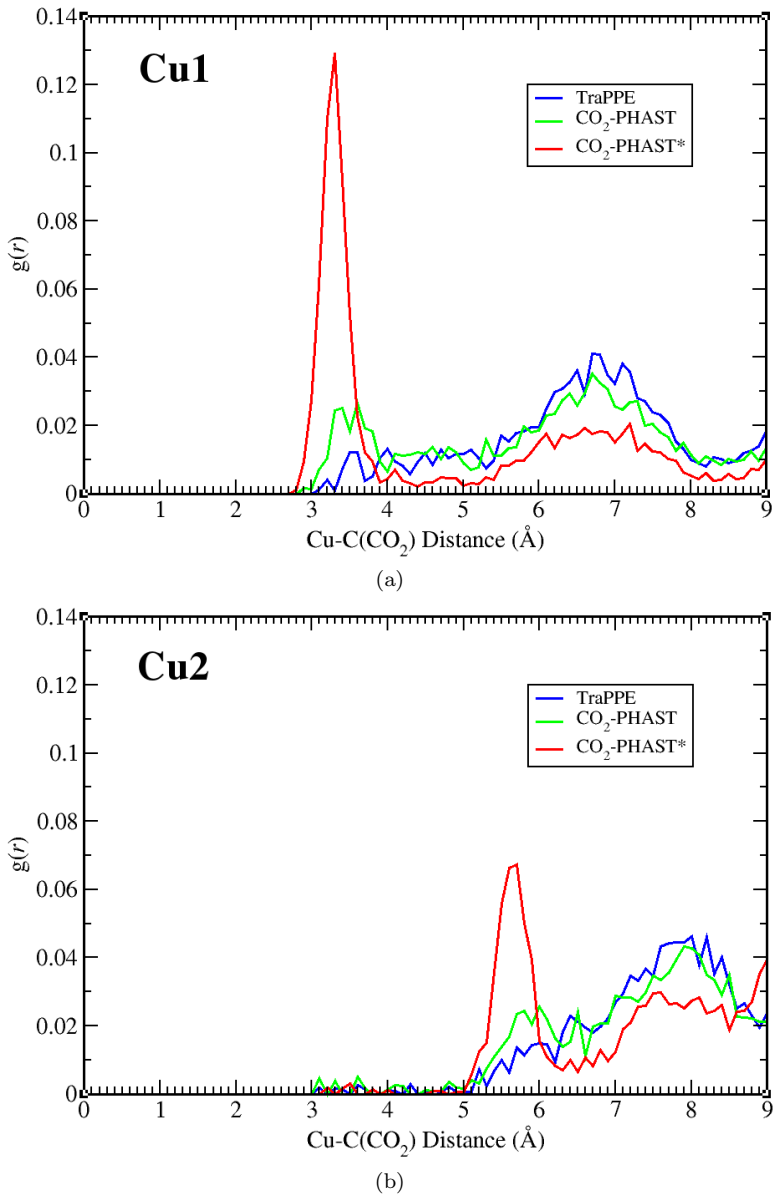


**Figure S6.** Radial distribution function (g($r$)) of $CO_2$ carbon atoms about **(a)** the Cu1 ions (atom label 1 in Figure S1) and **(b)** the Cu2 ions (atom label 2 in Figure S1) in UTSA-20 for simulations using the TraPPE (blue), $CO_2$-PHAST (green), and $CO_2$-PHAST* (red) models at 300 K and 0.01 atm.

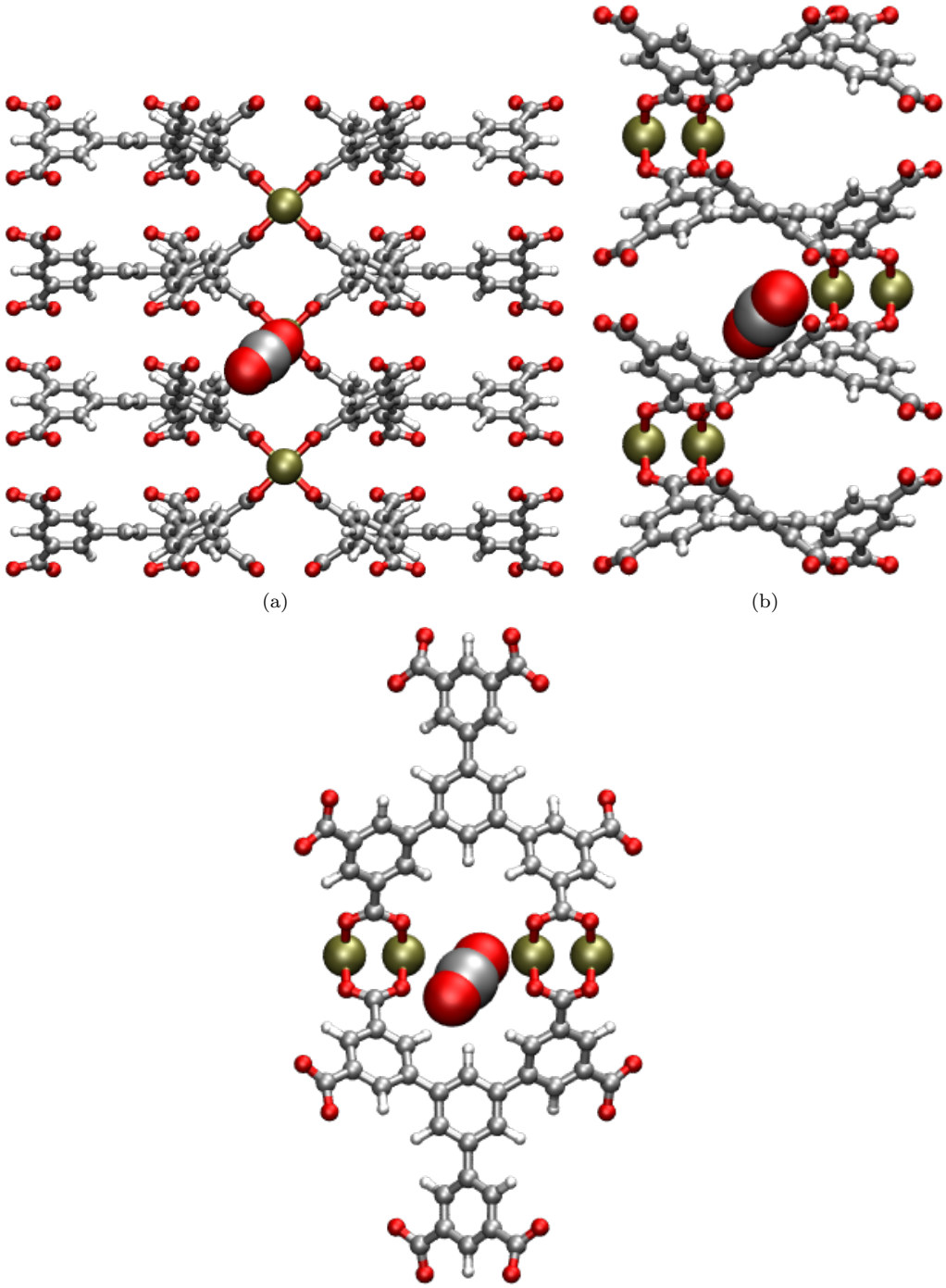


**Figure S7.** **(a)** The *a*-axis, **(b)** *b*-axis, and **(c)** *c*-axis view of a portion of the crystal structure of UTSA-20 showing a $CO_2$ molecule sorbed onto a Cu1 ion (atom label 1 in Figure S1) as determined from simulated annealing using the $CO_2$-PHAST* model. All views are orthographic projections. Atom colors: C = gray, H = white, O = red, Cu = tan.

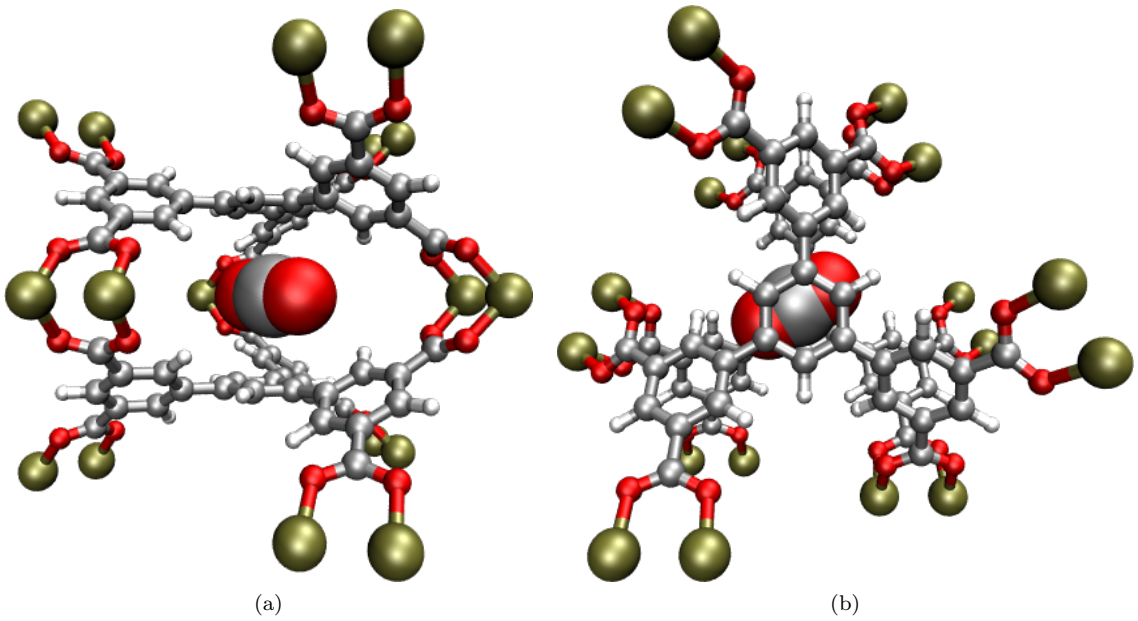


**Figure S8.** **(a)** The *b*-axis view and **(b)** *c*-axis view of a portion of the crystal structure of UTSA-20 showing a $CO_2$ molecule sorbed between two BHB linkers as determined from simulated annealing using the TraPPE and $CO_2$-PHAST models. Both views are perspective projections. Atom colors: C = gray, H = white, O = red, Cu = tan.

## Simulated $H_2$ Sorption Results

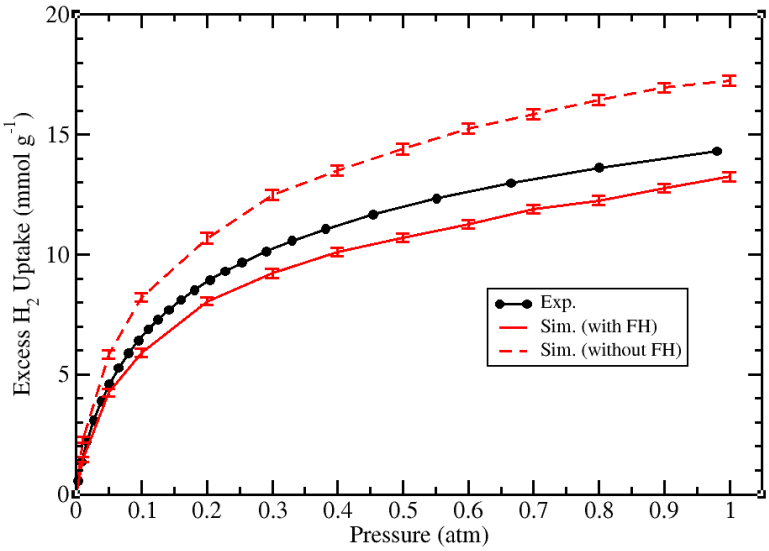


**Figure S9.** Low pressure excess $H_2$ sorption isotherms in UTSA-20 at 77 K for experiment (black) and simulations (red) with the inclusion of Feynman–Hibbs quantum corrections (solid)[15] and with the exclusion of such corrections (dashed). The experimental data were taken from reference 14.

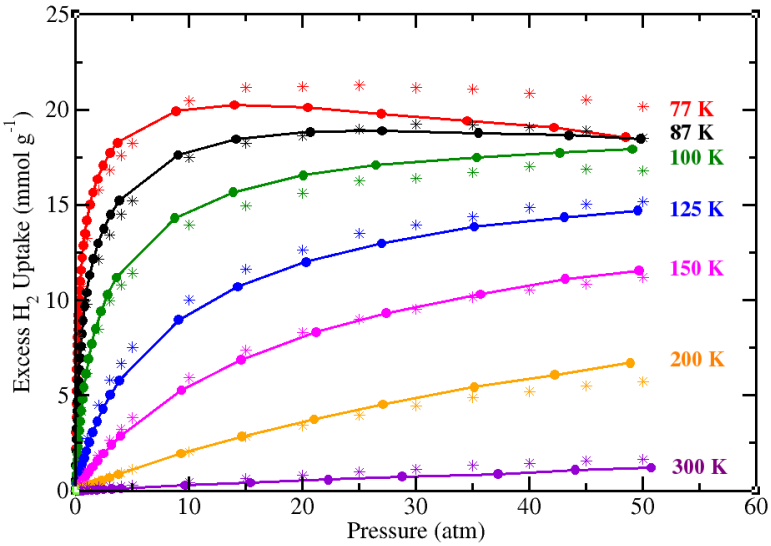


**Figure S10.** High pressure excess $H_2$ sorption isotherms in UTSA-20 for experiment (circles with lines) and simulation (star) at 77 (red), 87 (black), 100 (green), 125 (blue), 150 (magenta), 200 (orange), and 300 K (violet). Note, simulations at 77, 87, and 100 K were performed with Feynman–Hibbs quantum corrections,[15] while simulations at 125, 150, 200, and 300 K were performed without such corrections. The experimental data were taken from reference 14.

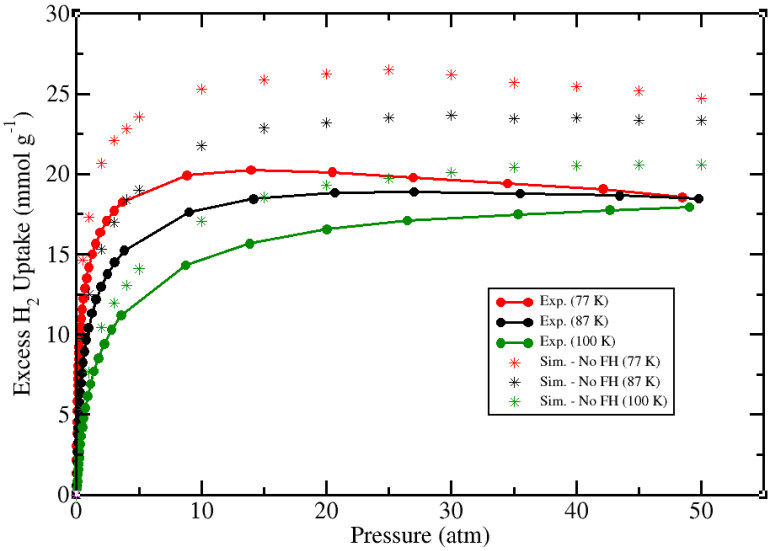


**Figure S11.** High pressure excess $H_2$ sorption isotherms in UTSA-20 for experiment (circles with lines) and simulation (star) at 77 (red), 87 (black), and 100 K (green) with the exclusion of Feynman–Hibbs quantum corrections.[15] The experimental data were taken from reference 14.

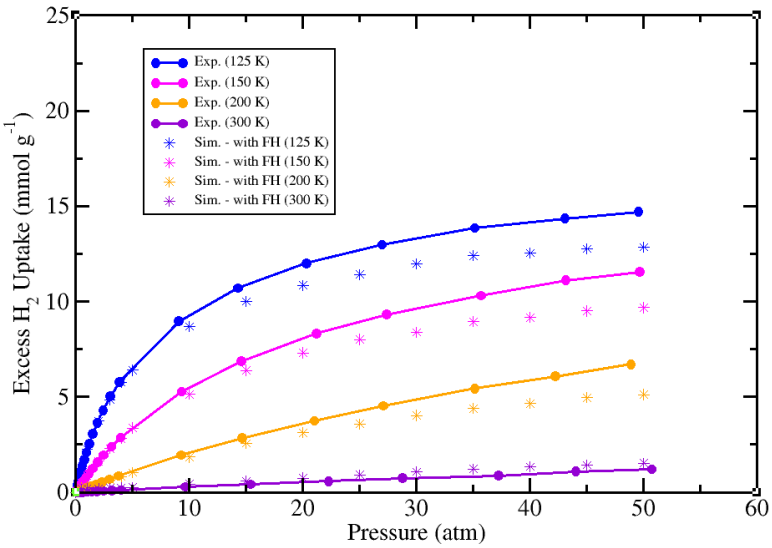


**Figure S12.** High pressure excess $H_2$ sorption isotherms in UTSA-20 for experiment (circles with lines) and simulation (star) at 125 (blue), 150 (magenta), 200 K (orange), and 300 K (violet) with the inclusion of Feynman–Hibbs quantum corrections.[15] The experimental data were taken from reference 14.

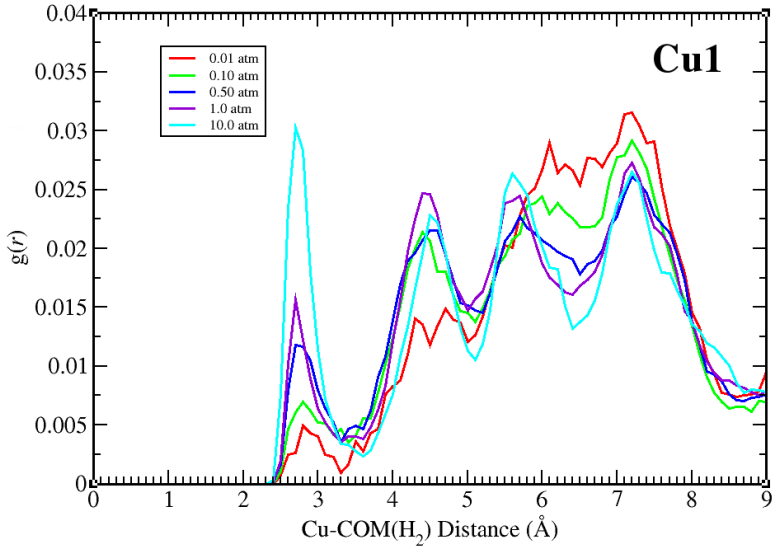


(a)

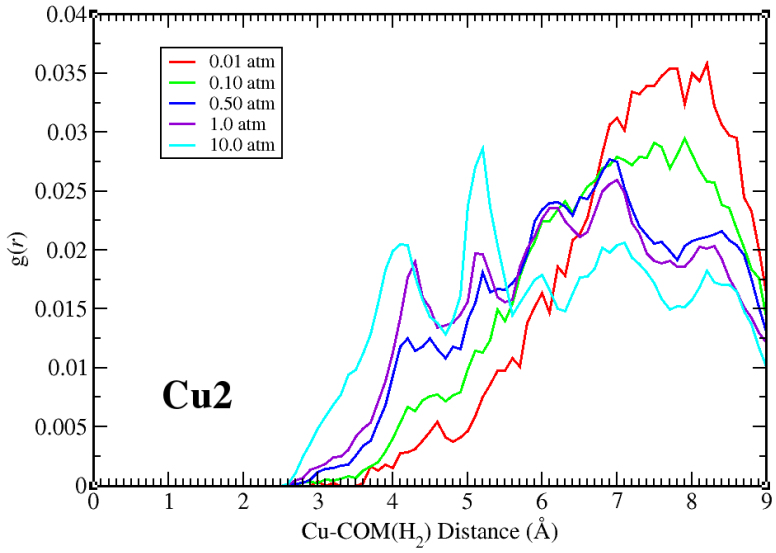


(b)

**Figure S13.** Radial distribution function (g($r$)) of the center-of-mass (COM) of $H_2$ molecules about **(a)** the Cu1 ions (atom label 1 in Figure S1) and **(b)** the Cu2 ions (atom label 2 in Figure S1) in UTSA-20 for simulations at 77 K and 0.01 (red), 0.10 (green), 0.50 (blue), 1.0 (violet), and 10.0 atm (cyan).

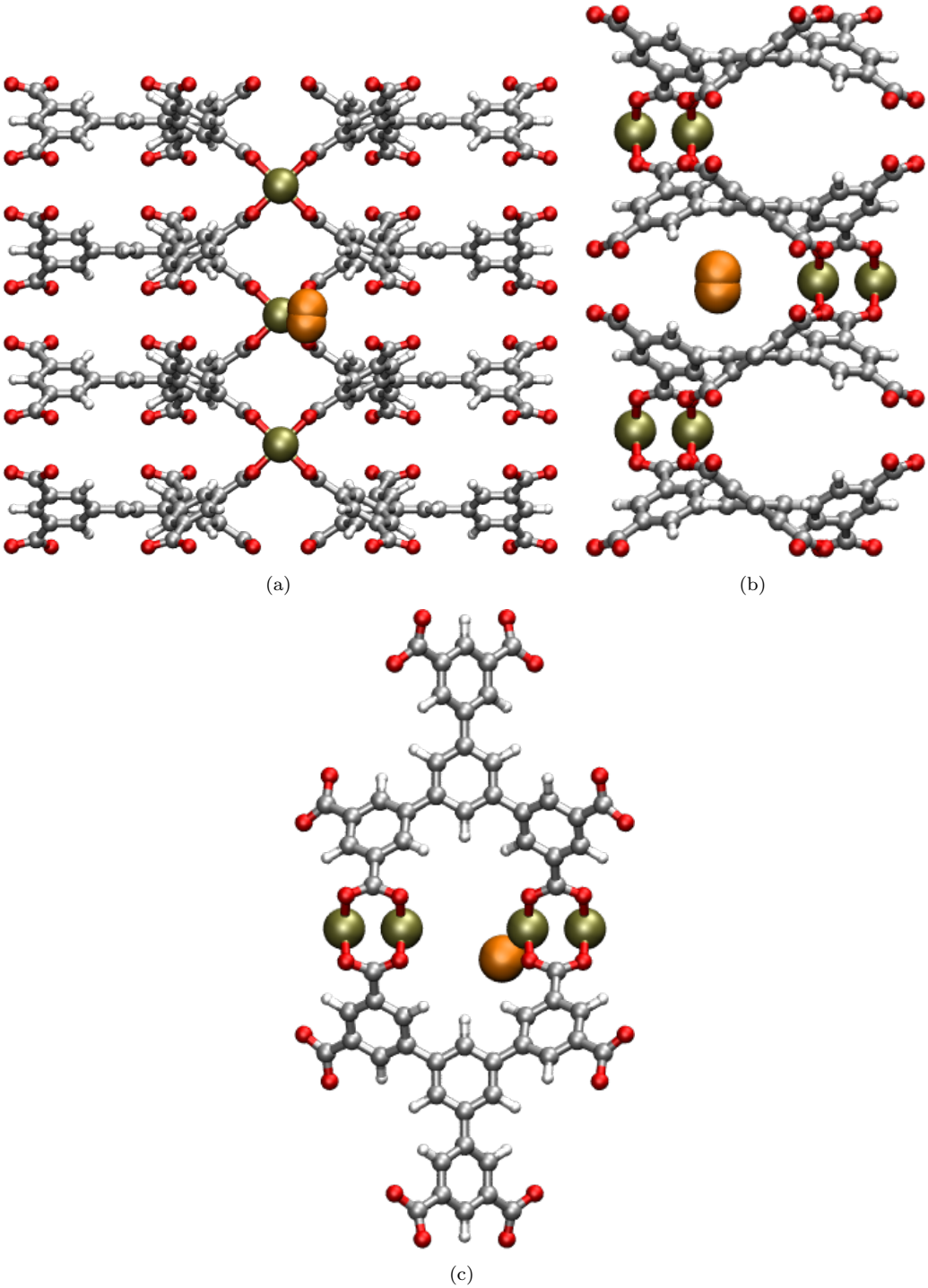


**Figure S14.** **(a)** The *a*-axis, **(b)** *b*-axis, and **(c)** *c*-axis view of a portion of the crystal structure for UTSA-20 showing a $H_2$ molecule (orange) sorbed within the small pores of the framework and proximal to two BHB linkers as determined from simulated annealing. All views are orthographic projections. Atom colors: C = gray, H = white, O = red, Cu = tan.

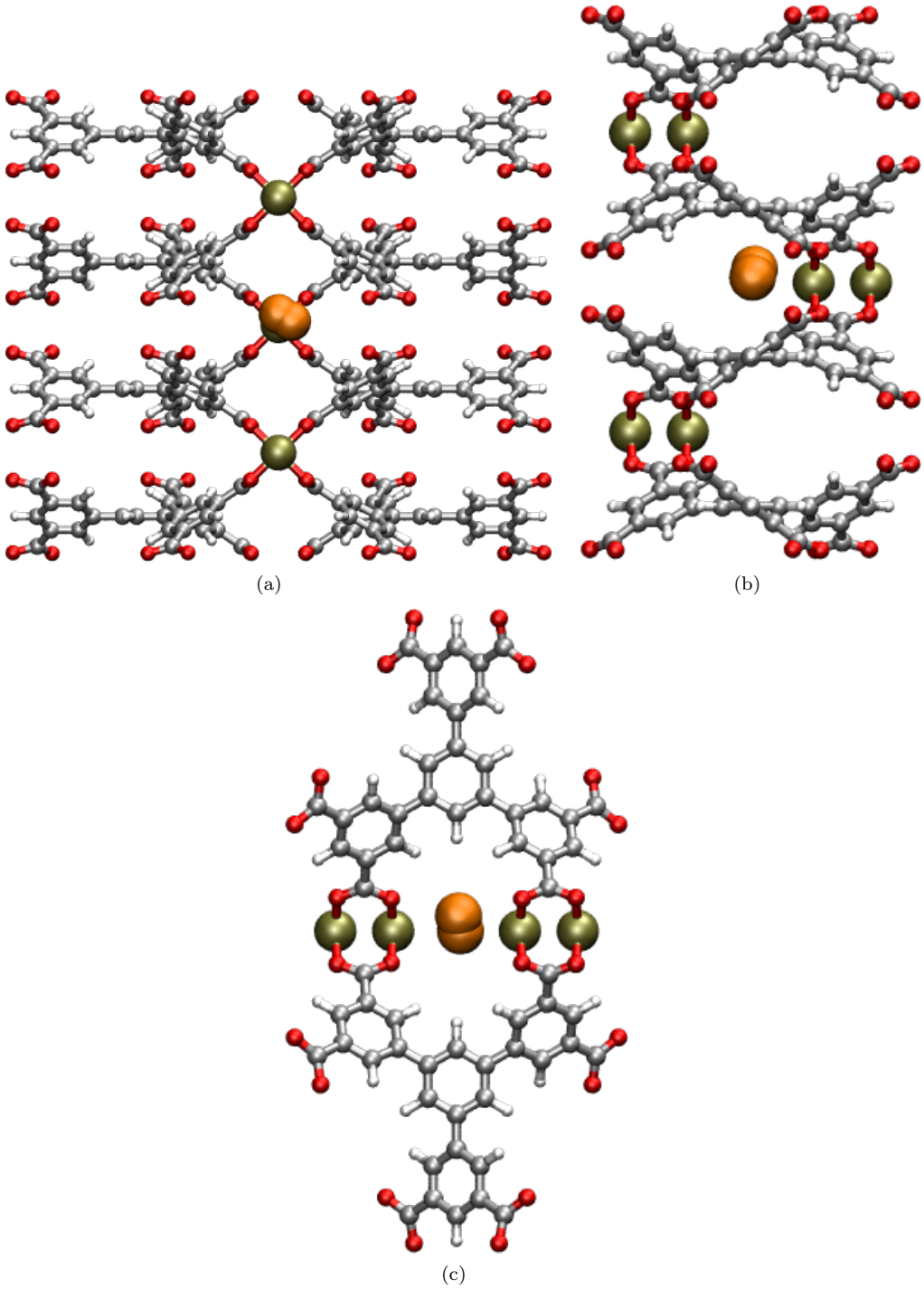


**Figure S15.** **(a)** The *a*-axis, **(b)** *b*-axis, and **(c)** *c*-axis view of a portion of the crystal structure for UTSA-20 showing a $H_2$ molecule (orange) sorbed onto a Cu1 ion (atom label 1 in Figure S1) as determined from GCMC simulations. All views are orthographic projections. Atom colors: C = gray, H = white, O = red, Cu = tan.

[1] M. Valiev, E. Bylaska, N. Govind, K. Kowalski, T. Straatsma, H. V. Dam, D. Wang, J. Nieplocha, E. Apra, T. Windus and W. de Jong, *Comput. Phys. Commun.*, 2010, **181**, 1477–1489.

[2] W. D. Cornell, P. Cieplak, C. I. Bayly, I. R. Gould, K. M. Merz, D. M. Ferguson, D. C. Spellmeyer, T. Fox, J. W. Caldwell and P. A. Kollman, *J. Am. Chem. Soc.*, 1995, **117**, 5179–5197.

[3] W. J. Stevens, H. Basch and M. Krauss, *J. Chem. Phys.*, 1984, **81**, 6026–6033.

[4] P. J. Hay and W. R. Wadt, *J. Chem. Phys.*, 1985, **82**, 270–283.

[5] L. A. LaJohn, P. A. Christiansen, R. B. Ross, T. Atashroo and W. C. Ermler, *J. Chem. Phys.*, 1987, **87**, 2812–2824.

[6] C. M. Breneman and K. B. Wiberg, *J. Comput. Chem.*, 1990, **11**, 361–373.

[7] L. Czepirski and J. JagieŁŁo, *Chem. Eng. Sci.*, 1989, **44**, 797–801.

[8] M. Dincă, A. Dailly, Y. Liu, C. M. Brown, D. A. Neumann and J. R. Long, *J. Am. Chem. Soc.*, 2006, **128**, 16876–16883.

[9] R Development Core Team, *R: A Language and Environment for Statistical Computing*, R Foundation for Statistical Computing, Vienna, Austria, 2008.

[10] B. Li, Y. Zhang, R. Krishna, K. Yao, Y. Han, Z. Wu, D. Ma, Z. Shi, T. Pham, B. Space, J. Liu, P. K. Thallapally, J. Liu, M. Chrzanowski and S. Ma, *J. Am. Chem. Soc.*, 2014, **136**, 8654–8660.

[11] S. D. Burd, S. Ma, J. A. Perman, B. J. Sikora, R. Q. Snurr, P. K. Thallapally, J. Tian, L. Wojtas and M. J. Zaworotko, *J. Am. Chem. Soc.*, 2012, **134**, 3663–3666.

[12] H. Pan, J. A. Ritter and P. B. Balbuena, *Langmuir*, 1998, **14**, 6323–6327.

[13] T. J. Ypma, *SIAM Rev.*, 1995, **37**, 531–551.

[14] Z. Guo, H. Wu, G. Srinivas, Y. Zhou, S. Xiang, Z. Chen, Y. Yang, W. Zhou, M. O'Keeffe and B. Chen, *Angew. Chem. Int. Ed.*, 2011, **50**, 3178–3181.

[15] R. P. Feynman and A. R. Hibbs, *Quantum Mechanics and Path Integrals*, McGraw-Hill, New York, 1965.